



# OPEN Multilayer network analysis in patients with end-stage kidney disease

Jiyae Yi<sup>1,5</sup>, Chang Min Heo<sup>1,5</sup>, Bong Soo Park<sup>1</sup>, Yoo Jin Lee<sup>1</sup>, Sihyung Park<sup>1</sup>, Yang Wook Kim<sup>1</sup>, Dong Ah Lee<sup>2</sup>, Kang Min Park<sup>2</sup>, Jinseung Kim<sup>3</sup> & Jung-hae Ko<sup>4</sup>✉

This study aimed to investigate alterations in a multilayer network combining structural and functional layers in patients with end-stage kidney disease (ESKD) compared with healthy controls. In all, 38 ESKD patients and 43 healthy participants were prospectively enrolled. They exhibited normal brain magnetic resonance imaging (MRI) without any structural lesions. All participants, both ESRD patients and healthy controls, underwent T1-weighted imaging, diffusion tensor imaging (DTI), and resting-state functional MRI (rs-fMRI) using the same three-tesla MRI scanner. A structural connectivity matrix was generated using the DTI and DSI programs, and a functional connectivity matrix was created using the rs-fMRI and SPM programs in the CONN toolbox. Multilayer network analysis was conducted based on structural and functional connectivity matrices using BRAPH. Significant differences were observed at the global level in the multilayer network between patients with ESKD and healthy controls. The weighted multiplex participation was lower in patients with ESKD than in healthy controls (0.6454 vs. 0.7212, adjusted  $p = 0.049$ ). However, other multilayer network measures did not differ. The weighted multiplex participation in the right subcentral gyrus, right opercular part of the inferior frontal gyrus, right occipitotemporal medial lingual gyrus, and right postcentral gyrus in patients with ESKD was lower than that in the corresponding regions in healthy controls (0.6704 vs. 0.8562, 0.8593 vs. 0.9388, 0.7778 vs. 0.8849, and 0.6825 vs. 0.8112; adjusted  $p < 0.05$ , respectively). This study demonstrated that the multilayer network combining structural and functional layers in patients with ESKD was different from that in healthy controls. The specific differences in weighted multiplex participation suggest potential disruptions in the integrated communication between different brain regions in these patients.

**Keywords** Neural networks, Connectome, Magnetic resonance imaging

End-stage kidney disease (ESKD) is of paramount importance to global public health owing to its diverse complications. ESKD is denoted by a glomerular filtration rate (GFR) persistently below 15 ml/min/1.73 m<sup>2</sup> for a duration exceeding three months<sup>1,2</sup>. Neurological complications of ESKD are widely recognized as common concerns, and they encompass conditions such as insomnia, depression, encephalopathy, stroke, and restless leg syndrome. These complications manifest as a diverse range of symptoms and can vary significantly in severity<sup>3,4</sup>. These complications can arise as a result of several factors, including uremic toxins, electrolyte imbalances (such as hyperkalemia), metabolic disturbances, vascular changes, and effects of dialysis<sup>4,5</sup>.

Numerous trials have been conducted to elucidate the underlying pathophysiology of neurological complications in patients with ESKD. Significant advancements in brain imaging modalities have complemented these efforts. Several studies have concluded that there is general cerebral atrophy and prominent lesions in the frontal lobes, based on brain imaging, including magnetic resonance imaging (MRI) and computed tomography (CT) scans<sup>6,7</sup>. Some studies have demonstrated white matter lesions, such as decreased deep white matter volume and hyperintensities, which are indicative of small vessel disease, as observed on brain MRI<sup>8,9</sup>.

Recently, there has been a notable surge in interest in graph theory-based research on brain connectivity. This approach offers a comprehensive framework for analyzing the intricate networks formed by both structural and

<sup>1</sup>Departments of Internal Medicine, Haeundae Paik Hospital, Inje University College of Medicine, Busan, South Korea. <sup>2</sup>Departments of Neurology, Haeundae Paik Hospital, Inje University College of Medicine, Busan, South Korea. <sup>3</sup>Department of Family Medicine, Busan Paik Hospital, Inje University College of Medicine, Busan, Republic of Korea. <sup>4</sup>Department of Internal Medicine, Haeundae Paik Hospital, Inje University College of Medicine, Haeundae-ro 875, Haeundae-gu, Busan 48108, Republic of Korea. <sup>5</sup>These authors contributed equally: Jiyae Yi and Chang Min Heo. ✉email: arrioph1@gmail.com

functional connectivity in the brain<sup>10</sup>. Consequently, there has been a growing effort to clarify the neurological complications in patients with ESKD. In one study, neural tract lesions in patients with ESKD were identified based on diffusion tensor imaging (DTI) findings<sup>11</sup>. Some studies have reported alterations in white matter integrity and connectivity among patients with ESKD, as evidenced by lower fractional anisotropy (FA) and higher mean diffusivity (MD)<sup>12–15</sup>. A previous study showed significantly lower functional connectivity in hemodialysis-dependent patients with ESKD, especially in the frontal lobe, which is strongly associated with neurocognitive dysfunction<sup>16</sup>. Several studies using resting-state functional MRI (rs-fMRI) have provided evidence indicating a disturbance of typical global integration within brain networks, characterized by a diminished clustering coefficient and global efficiency, alterations in small-worldness, and a heightened characteristic path length in patients with ESKD<sup>15–18</sup>.

Graph theory has ignited a surge of interest in multilayer networks in the domain of brain neuroscience by incorporating various layers such as structural and functional layers within the brain<sup>19–21</sup>. The brain's network can be better understood and explained by performing multilayer analysis rather than a simple unilayer analysis, and the structural and functional networks are not separated but closely related to each other. Furthermore, by integrating multimodal data, a comprehensive understanding of the brain can be achieved, while also capturing temporal changes in brain dynamics<sup>22,23</sup>. Recently, brain multilayer network analysis has been conducted to understand the pathophysiology of various neurological disorders. Using multilayer network analysis, one study demonstrated a diminished loss of inter-frequency centrality in memory-related association areas in patients with Alzheimer's disease<sup>2</sup>. Other studies have shown significant changes between the multilayer networks of patients with migraine and those of healthy controls<sup>24</sup>. Multilayer network analysis in patients with post-traumatic stress syndrome show reduced switching rates in brain functional network modules at global, sub-network, and nodal levels<sup>25</sup>.

However, studies on multilayered networks in patients with ESKD are currently scarce. This study aimed to investigate alterations in a multilayer network combining structural and functional layers in patients with ESKD compared with healthy controls.

## Methods

### Participants

This prospective study was approved by the Institutional Review Board (IRB) of Haeundae Paik Hospital, and all methods were performed in accordance with the guidelines and regulations (IRB number: 2018-09-015-003). Informed consent was obtained from all participants before participation. In all, 38 patients with ESKD and a glomerular filtration rate < 15 mL/min/1.73 m<sup>2</sup> were prospectively enrolled. All patients with ERKD were undergoing dialysis. All the enrolled patients exhibited normal brain MRI findings without any structural lesions at the time of inclusion. We also enrolled 43 age- and sex-matched healthy participants with no previous history of any medical or neurological disease as a control group. Furthermore, the brain MRIs of these participants revealed no structural lesions.

### MRI acquisition

All participants, both ESKD patients and healthy controls, underwent T1-weighted imaging, DTI, and rs-fMRI using the same three-tesla MRI scanner (Achieva Tx; Phillips Healthcare). DTI was performed using spin-echo single-shot echo-planar pulse sequences with 32 diffusion directions (repetition time/time to echo = 8620/85 ms, flip angle = 90°, slice thickness = 2.25 mm, acquisition matrix = 120 × 120, field of view = 240 × 240 mm<sup>2</sup>, and *b*-value = 1,000 s/mm<sup>2</sup>). The rs-fMRI was performed using multi-slice echo-planar imaging sequences (Repetition time/Time to echo = 3000/30 ms, Flip angle = 65°, slice thickness = 4.4 mm, acquisition matrix = 128 × 128, Field of view = 220 × 220 mm<sup>2</sup>, scan time = 7 min 30 s).

### Multilayer network analysis

First, a structural connectivity matrix was generated for individual participants using the DSI program. Raw DTI data were preprocessed in the DSI program, with the help of image distortion and artifact correction, as well as image intensity normalization. Diffusion tensors were computed using a generalized Q-sampling imaging method at each voxel in the brain, and the fiber orientation distribution function was employed to estimate white matter fiber orientation. A deterministic tractography algorithm was applied to reconstruct white matter fiber tracts between different brain regions, resulting in a structural connectivity matrix. A total of 150 nodes in this matrix represented the regions of interest (Suppl. 1) and the edges represented the number of fiber tracts connecting each region. Second, a functional connectivity matrix was created using the SPM program (version 12) and the CONN toolbox (version 22a). Raw fMRI data were preprocessed using the SPM program. The detailed process was described in our previous work<sup>26</sup>. Regions of interest were defined in a manner similar to that used when creating the structural matrix, and a functional connectivity matrix was in individual participants.

Third, a multilayer network analysis was conducted based on structural and functional connectivity matrices using the BRAPH program (version 2). The detailed process was also described in our previous work<sup>26</sup>. The analysis involved a comparison of the two participant groups using connectivity-functional multiplex data and weighted undirected graphs. Various network measures were calculated at the global level, including weighted multiplex participation, persistence, average overlapping strength, average multiplex participation, average multilayer clustering, multilayer modularity, and average flexibility. Weighted multiplex participation was the nodal homogeneity of the number of neighbors across layers. Persistence was calculated as the normalized sum of the number of nodes that did not change their community assignments. The average overlapping strength was the average sum of the strengths of a node in all layers. The average multiplex participation indicated the nodal homogeneity of the number of neighbors of a node across layers. Average multilayer clustering was the average of the two-layer clustering coefficients for all nodes. The clustering coefficient was the fraction of the triangles

around a node. Multilayer modularity was the quality of the resulting partitions in a multilayer network. Average flexibility is the average flexibility of all the nodes in a multilayer network. The flexibility of each node was calculated as the number of times it changed the community assignment, normalized by the total possible number of changes.

Finally, the network measures were compared between patients with ESKD and healthy controls. In case of significant differences at the global level in multilayer network analysis, the nodal level of the multilayer network was also analyzed. The multilayer network process is illustrated in Fig. 1.

### Statistical analysis

The demographic characteristics of patients with ESKD and healthy controls were assessed using an independent t-test and chi-square test using MedCalc Statistical Software version 20.014 (MedCalc Software Ltd, Ostend, Belgium; <https://www.medcalc.org>; 2021). Network measures in the multilayer network analysis were compared between groups using a permutation test integrated into the BRAPH program. Statistical significance was set at  $p$ -value  $< 0.05$ . For comparisons at both global and nodal levels in the multilayer network analysis, an adjusted  $p$ -value was calculated by applying multiple corrections using the false discovery rate (Benjamini-Hochberg procedure)<sup>27–30</sup>.

## Results

### Participants

Table 1 shows the demographic characteristics of patients with ESKD and healthy controls. There were no differences in the demographic characteristics between patients with ESKD and healthy controls. The ages in the two groups were  $61.7 \pm 6.8$  vs.  $60.0 \pm 7.8$ , and no statistically significant difference was found ( $p = 0.286$ ). Additionally, the male-to-female ratios were 45% vs. 42%, with no difference between the two groups ( $p = 0.794$ ).

### Global level of multilayer network analysis

Table 2 shows the results of the global level of multilayer network analysis. There were significant differences at the global level in the multilayer network between patients with ESKD and healthy controls. The weighted multiplex participation was lower in patients with ESKD than in healthy controls (0.6454 vs. 0.7212, adjusted  $p = 0.049$ ). However, other multilayer network measures, including persistence, average overlapping strength, average multiplex participation, average multilayer clustering, multilayer modularity, and average flexibility, did not differ.

### Nodal level of multilayer network analysis

Figure 2 shows the nodes demonstrating significant differences in the weighted multiplex participation between patients with ESKD and healthy controls. The weighted multiplex participation in the right subcentral gyrus,

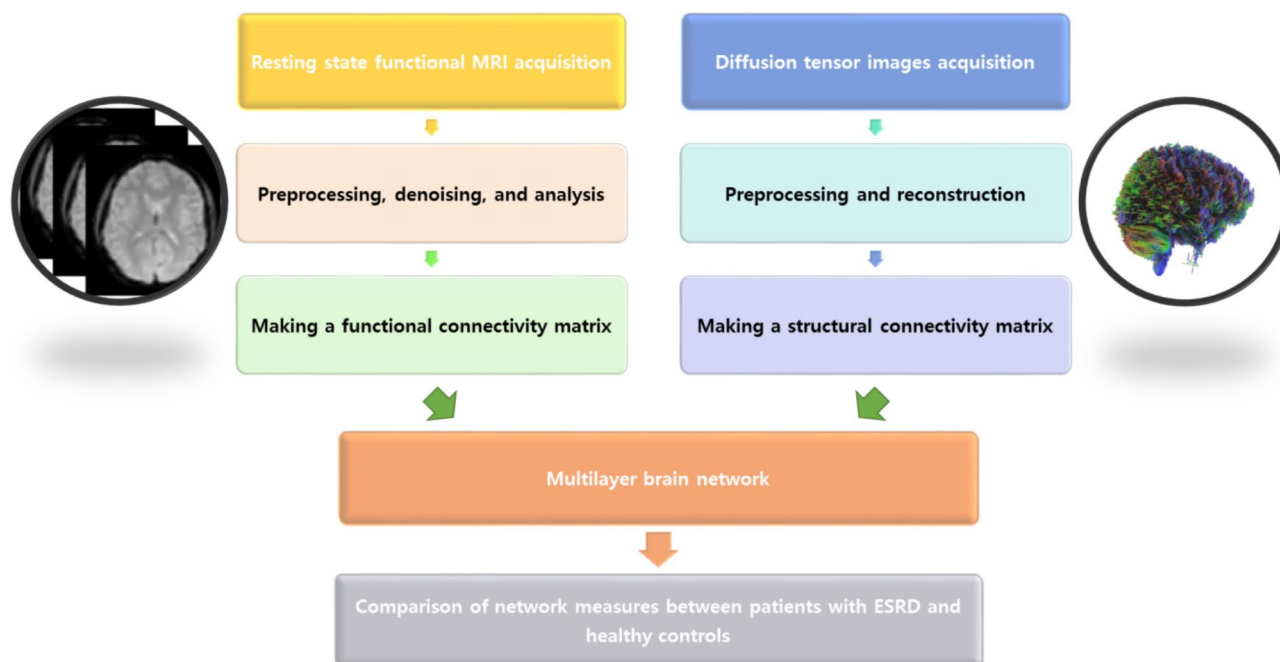


**Fig. 1.** Process of multilayer network analysis. A functional connectivity matrix was created using the SPM program and CONN toolbox based on resting-state functional MRI, and a structural connectivity matrix was generated using a DSI program based on diffusion tensor imaging. Subsequently, a multilayer network analysis was conducted based on the structural and functional connectivity matrices using the BRAPH program. Finally, multilayer network measures were compared between patients with ESRD and healthy controls.

Variables	Patients with ESKD (N = 38)	Healthy controls (N = 43)	p-value
Demographic data			
Age, years	61.7 ± 6.8	60.0 ± 7.8	0.286
Sex, male	17 (45)	18 (42)	0.794
Hemodialysis	19 (50)		
Peritoneal dialysis	19 (50)		
Kt/V	1.86 ± 0.5		
Dialysis duration, month	47.9 ± 50.6		
Laboratory data			
Hemoglobin, g/dL	10.5 ± 1.1		
Hematocrit, %	32.2 ± 3.6		
Protein, g/dL	6.5 ± 0.6		
Albumin, d/dL	3.8 ± 0.4		
BUN, mg/dL	57.3 ± 17.2		
Creatinine, mg/dL	9.0 ± 2.6		
Sodium, mmol/L	139.0 ± 3.3		
Potassium, mmol/L	4.7 ± 0.7		
Chloride, mmol/L	99.6 ± 4.1		
Calcium, mg/dL	8.5 ± 0.8		
Phosphate, mg/dL	4.5 ± 0.9		
Parathyroid hormone, pg/mL	268.4 ± 210.5		
Total CO <sub>2</sub> contents, mmol/L	24.2 ± 4.7		

**Table 1.** Demographic and clinical characteristics of patients with ESKD and healthy controls. Data are presented as number (%) or mean ± standard deviation. ESKD end-stage kidney disease, Kt/V dialyzer clearance; time/distribution volume of urea, BUN blood urea nitrogen.

	Patients with ESKD	Controls	Difference	Lower value of the 95% confidence interval	Upper value of the 95% confidence interval	p-value	adjusted p-value
Weighted multiplex participation	0.6454	0.7212	0.0758	-0.0128	0.0112	0.013	*0.048
Persistence	0.4425	0.4526	0.0101	-0.0348	0.0311	0.199	0.337
Average overlapping strength	34.2239	34.5994	0.3755	-1.6153	1.5247	0.241	0.337
Average multiplex participation	0.7454	0.7245	-0.021	-0.0128	0.0112	0.016	0.056
Average multiplex clustering	0.1547	0.1551	0.0004	-0.0095	0.0091	0.353	0.353
Multilayer modularity	0.3961	0.3804	-0.0157	-0.0147	0.0141	0.036	0.084
Average flexibility	0.5516	0.555	0.0035	-0.0382	0.0353	0.347	0.353

**Table 2.** Results of the multilayer network analysis at the global level. \*Indicates statistical significance ( $p < 0.05$ ).

right opercular part of the inferior frontal gyrus, right occipitotemporal medial lingual gyrus, and right postcentral gyrus among patients with ESKD was lower than that in the corresponding regions among healthy controls (right subcentral gyrus, 0.6704 vs. 0.8562; right opercular part of the inferior frontal gyrus, 0.8593 vs. 0.9388; right occipitotemporal medial lingual gyrus, 0.7778 vs. 0.8849; and right postcentral gyrus, 0.6825 vs. 0.8112; adjusted  $p < 0.05$ , respectively).

## Discussion

The present study aimed to investigate alterations in the multilayer network combining structural and functional layers between patients with ESKD and healthy controls. Numerous attempts have been made to explain the use of multilayer network analysis in many neurological disorders; however, there have been no approaches using multilayer networks in patients with ESKD<sup>2,24,25</sup>. Our study revealed a significant reduction in weighted multiplex participation at both the global and nodal levels among patients with ESKD compared with healthy controls. Furthermore, examination at the nodal level identified several specific brain regions characterized by decreased weighted multiplex participation, highlighting localized deficits in the interlayer interactions within the brain network of patients with ESKD.

At the global level, weighted multiplex participation was lower in patients with ESKD than in healthy controls. Weighted multiplex participation is a quantitative measure of a node's involvement across multiple network

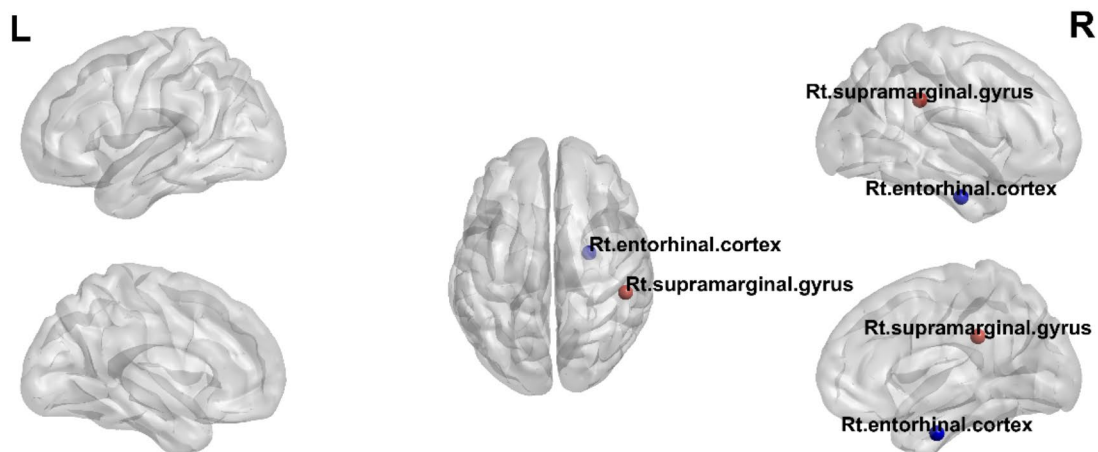


**Fig. 2.** Nodes demonstrating significant differences in the weighted multiplex participation between patients with ESRD and healthy controls. The red circles show regions with decreased weighted multiplex participation in patients with ESRD compared with healthy controls; these regions include the right subcentral gyrus, right opercular part of the inferior frontal gyrus, right occipitotemporal medial lingual gyrus, and right postcentral gyrus.

layers determined by evaluating the weighted interactions within each layer<sup>31–35</sup>. Therefore, decreased weighted multiplex participation suggests a diminished level of integration or engagement of brain regions across the structural and functional layers of connectivity in patients with ESKD. This result corresponds to the finding of a deficit in integration within multilayer networks among patients with Alzheimer’s disease and mild cognitive disorders<sup>35</sup>.

Additional analysis was conducted at the nodal level of the multilayer network, revealing a decrease in weighted multiplex participation within specific regions, such as the right subcentral gyrus, right opercular part of the inferior frontal gyrus, right occipito-temporal medial lingual gyrus, and right postcentral gyrus, in patients with ESKD compared with healthy controls. The right subcentral gyrus plays a crucial role in sensorimotor integration; somatosensory processing; language and speech; and motor coordination<sup>36,37</sup>. The right postcentral gyrus, located on the lateral surface of the anterior parietal lobe, plays a role in somatosensory processing and sensorimotor integration<sup>37,38</sup>. The right opercular part of the inferior frontal gyrus is important for language production, executive functioning, and motor control<sup>37,39</sup>. The right occipitotemporal medial lingual gyrus plays a role in visual processing and word and face recognition<sup>37,40</sup>. These findings suggest the possibility that the complementary relationship between structural and functional networks in these nodes had decreased.

Previously, the dominant cerebral hemisphere, which mainly refers to the left side of a left-handed person, was known to play a crucial role in brain function. However, recent research has revealed the importance of the non-dominant cerebral hemisphere, primarily referring to the right side, in brain function. The non-dominant hemisphere plays a significant role in primary cognitive functions, such as visuospatial and social cognition<sup>41</sup>. The white matter fiber tract, known as the superior longitudinal fasciculus in the perisylvian area of the right hemisphere, plays a crucial role in cognitive function. The subcentral, inferior frontal, and postcentral gyri, which showed significant changes in this study, correspond to these regions. Accordingly, damage to the multilayer network in these areas may be related to neurological impairments in patients with ESKD. These regions are distinct areas with diverse functions; however, they have interconnected neural networks and functional relationships. Further research utilizing multilayer network analysis may provide valuable insights into the pathophysiology of neurological complications in patients with ESKD, and inform targeted interventions to mitigate these adverse outcomes.

Our study represents the first attempt to conduct a multilayer network analysis in patients with ESKD; however, it has several limitations. First, this study was planned at a single center, and the relatively small sample size is a limitation. This may have led to a selection bias, and we believe that larger-scale studies are necessary in the future. Second, we conducted a multilayer network analysis of patients with ESKD at a group level rather than at an individual level. Therefore, we could not perform a correlation analysis between clinical data and the multilayer network. Third, cognitive function tests were not performed. This represents a limitation in understanding the relationship between cognitive function impairment in patients with ESKD and variables within the multilayer network. Despite these limitations, this study demonstrates the value of multilayer network

analysis in understanding the pathophysiology of neurological complications in patients with ESKD and its potential for diverse future applications.

## Conclusion

This study demonstrated that the multilayer network combining structural and functional layers differs between patients with ESKD and healthy controls. The specific differences in weighted multiplex participation suggest potential disruptions in integrated communication between different brain regions in patients with ESKD.

## Data availability

The datasets used and/or analysed during the current study available from the corresponding author on reasonable request.

Received: 10 May 2024; Accepted: 21 November 2024

Published online: 30 December 2024

## References

- Levey, A. S. et al. Definition and classification of chronic kidney disease: a position statement from kidney disease: improving global outcomes (KDIGO). *Kidney Int.* **67**(6), 2089–2100 (2005).
- Guillon, J. et al. Loss of brain inter-frequency hubs in Alzheimer's disease. *Sci. Rep.* **7**(1), 10879 (2017).
- Brouns, R. & De Deyn, P. P. Neurological complications in renal failure: a review. *Clin. Neurol. Neurosurg.* **107**(1), 1–16 (2004).
- Bronas, U. G., Puzantian, H. & Hannan, M. Cognitive impairment in chronic kidney disease: vascular milieu and the potential therapeutic role of Exercise. *Biomed. Res. Int.* **2017**, 2726369 (2017).
- Liabeuf, S. et al. Chronic kidney disease and neurological disorders: are uraemic toxins the missing piece of the puzzle? *Nephrol. Dial. Transpl.* **37**(Suppl 2), ii33–ii44 (2021).
- Passer, J. A. Cerebral atrophy in end-stage uremia. *Proc. Clin. Dial. Transpl. Forum* **7**, 91–94 (1977).
- Kamata, T. et al. Morphologic abnormalities in the brain of chronically hemodialyzed patients without cerebrovascular disease. *Am. J. Nephrol.* **20**(1), 27–31 (2000).
- Cho, A. H. et al. Impaired kidney function and cerebral microbleeds in patients with acute ischemic stroke. *Neurology* **73**(20), 1645–1648 (2009).
- Ikram, M. A. et al. Kidney function is related to cerebral small vessel disease. *Stroke* **39**(1), 55–61 (2008).
- Hallquist, M. N. & Hillary, F. G. Graph theory approaches to functional network organization in brain disorders: a critique for a brave new small-world. *Netw. Neurosci.* **3**(1), 1–26 (2018).
- Kim, H. S. et al. Diffusion tensor imaging findings in neurologically asymptomatic patients with end stage renal disease. *NeuroRehabilitation* **29**(1), 111–116 (2011).
- Chen, H. J., Zhang, L. J. & Lu, G. M. Multimodality MRI findings in patients with end-stage renal disease. *Biomed. Res. Int.* **2015**, 697402 (2015).
- Chou, M. C. et al. Widespread white matter alterations in patients with end-stage renal disease: a voxelwise diffusion tensor imaging study. *AJNR Am. J. Neuroradiol.* **34**(10), 1945–1951 (2013).
- Zhang, R. et al. Reduced white matter integrity and cognitive deficits in maintenance hemodialysis ESRD patients: a diffusion-tensor study. *Eur. Radiol.* **25**(3), 661–668 (2015).
- Park, B. S. et al. Alterations in structural and functional connectivities in patients with end-stage renal disease. *J. Clin. Neurol.* **16**(3), 390–400 (2020).
- Zheng, G. et al. Altered brain functional connectivity in hemodialysis patients with end-stage renal disease: a resting-state functionalMR imaging study. *Metab. Brain Dis.* **29**(3), 777–786 (2014).
- Lee, Y. J. et al. Alteration of brain connectivity in neurologically asymptomatic patients with chronic kidney disease. *Med. (Baltim).* **100**(16), e25633 (2021).
- Jin, M. et al. Altered resting-state functional networks in patients with hemodialysis: a graph-theoretical based study. *Brain Imaging Behav.* **15**(2), 833–845 (2021).
- Bullmore, E. & Sporns, O. Complex brain networks: graph theoretical analysis of structural and functional systems. *Nat. Rev. Neurosci.* **10**(3), 186–198 (2009).
- Sporns, O. Contributions and challenges for network models in cognitive neuroscience. *Nat. Neurosci.* **17**(5), 652–660 (2014).
- Park, K. M. et al. Alterations of functional connectivity in patients with restless legs syndrome. *J. Clin. Neurol.* **18**(3), 290–297 (2022).
- Fornito, A., Zalesky, A. & Breakspear, M. The connectomics of brain disorders. *Nat. Rev. Neurosci.* **16**(3), 159–172 (2015).
- Bassett, D. S. & Sporns, O. Network neuroscience. *Nat. Neurosci.* **20**(3), 353–364 (2017).
- Kim, J., Lee, D. A., Lee, H. J. & Park, K. M. Multilayer network changes in patients with migraine. *Brain Behav.* **13**(12), e3316 (2023).
- Suo, X. et al. Multilayer Network Analysis of Dynamic Network Reconfiguration in Adults With Posttraumatic Stress Disorder. *Biological Psychiatry: Cognitive Neuroscience and Neuroimaging.* **8**(4):452–61. (2023).
- Park, K. M., Kim, K. T., Lee, D. A., Motamedi, G. K. & Cho, Y. W. Structural and functional multilayer network analysis in restless legs syndrome patients. *J. Sleep. Res.* e14104. (2023).
- Yu, H., Si, G. & Si, F. Mendelian randomization validates the Immune Landscape mediated by Aggrephagy in Esophageal squamous cell carcinoma patients from the perspectives of multi-omics. *J. Cancer* **15**(7), 1940–1953 (2024).
- Yu, H., Ji, X. & Ouyang, Y. Unfolded protein response pathways in stroke patients: a comprehensive landscape assessed through machine learning algorithms and experimental verification. *J. Transl. Med.* **21**(1), 759 (2023).
- Yu, H. et al. Utilising Network Pharmacology to explore underlying mechanism of Astragalus membranaceus in improving Sepsis-Induced Inflammatory response by regulating the balance of IkBa and NF-κB in rats. *Evid. Based Complement. Alternat. Med.* **2022**, 7141767 (2022).
- Yu, H. & Song, X. The relationship between Alzheimer disease and thyroiditis: a two-sample mendelian randomization study. *Med. (Baltim).* **102**(44), e35712 (2023).
- Lee, D. A., Lee, H.-J. & Park, K. M. Involvement of the default mode network in patients with transient global amnesia: multilayer network. *Neuroradiology* **65**(12), 1729–1736 (2023).
- Puxeddu, M. G., Petti, M. & Astolfi, L. A comprehensive analysis of Multilayer Community Detection algorithms for application to EEG-Based brain networks. *Front. Syst. Neurosci.* **15**, 624183 (2021).
- Shahabi, H., Nair, D. R. & Leahy, R. M. Multilayer brain networks can identify the epileptogenic zone and seizure dynamics. *eLife* **12**, e68531 (2023).
- Casas-Roma, J. et al. Applying multilayer analysis to morphological, structural, and functional brain networks to identify relevant dysfunction patterns. *Netw. Neurosci.* **6** (3), 916–933 (2022).

35. Wang, X. et al. Deficit of cross-frequency integration in mild cognitive impairment and Alzheimer's Disease: a Multilayer Network Approach. *J. Magn. Reson. Imaging* **53**(5), 1387–1398 (2021).
36. McGlone, F. et al. Functional neuroimaging studies of human somatosensory cortex. *Behav. Brain. Res.* **135**(1), 147–158 (2002).
37. Ribas, G. C. The cerebral sulci and gyri. *Neurosurgical Focus FOC.* **28**(2), E2 (2010).
38. Kropf, E., Syan, S. K., Minuzzi, L. & Frey, B. N. From anatomy to function: the role of the somatosensory cortex in emotional regulation. *Braz J. Psychiatry* **41**(3), 261–269 (2019).
39. Hampshire, A., Chamberlain, S. R., Monti, M. M., Duncan, J. & Owen, A. M. The role of the right inferior frontal gyrus: inhibition and attentional control. *NeuroImage* **50**(3), 1313–1319 (2010).
40. Palejwala, A. H. et al. Anatomy and White Matter connections of the Lingual Gyrus and Cuneus. *World Neurosurg.* **151**, e426–e37 (2021).
41. Bernard, F., Lemée, J. M., Ter Minassian, A. & Menei, P. Right hemisphere cognitive functions: from clinical and anatomic bases to Brain Mapping during Awake Craniotomy Part I: clinical and functional anatomy. *World Neurosurg.* **118**, 348–359 (2018).

## Acknowledgements

We are grateful to the participants who generously volunteered their time and effort to take part in our study.

## Author contributions

Conceptualization, methodology and original draft preparation: KMP, BSP. Data collecting: SHP, CMH. Statistical analysis: YJL, DAL. Writing manuscript: YJY, CMH. Revising manuscript: YWK, JSK, JHK.

## Declarations

### Competing interests

The authors declare no competing interests.

### Additional information

**Supplementary Information** The online version contains supplementary material available at <https://doi.org/10.1038/s41598-024-80645-2>.

**Correspondence** and requests for materials should be addressed to J.K.

**Reprints and permissions information** is available at [www.nature.com/reprints](http://www.nature.com/reprints).

**Publisher's note** Springer Nature remains neutral with regard to jurisdictional claims in published maps and institutional affiliations.

**Open Access** This article is licensed under a Creative Commons Attribution-NonCommercial-NoDerivatives 4.0 International License, which permits any non-commercial use, sharing, distribution and reproduction in any medium or format, as long as you give appropriate credit to the original author(s) and the source, provide a link to the Creative Commons licence, and indicate if you modified the licensed material. You do not have permission under this licence to share adapted material derived from this article or parts of it. The images or other third party material in this article are included in the article's Creative Commons licence, unless indicated otherwise in a credit line to the material. If material is not included in the article's Creative Commons licence and your intended use is not permitted by statutory regulation or exceeds the permitted use, you will need to obtain permission directly from the copyright holder. To view a copy of this licence, visit <http://creativecommons.org/licenses/by-nc-nd/4.0/>.

© The Author(s) 2024